

Metadata of the chapter that will be visualized online

Chapter Title	Reliable Transmission Protocol for Underwater Acoustic Networks	
Copyright Year	2017	
Copyright Holder	Springer International Publishing AG	
Corresponding Author	Family Name	Du
	Particle	
	Given Name	Xiujuan
	Suffix	
	Division	School of Computer Science
	Organization	Qinghai Normal University
	Address	Xining, 810008, Qinghai, China
	Organization	Key Laboratory of the Internet of Things of Qinghai Province
	Address	Guinan, China
	Email	dxj@qhnu.edu.cn
Author	Family Name	Li
	Particle	
	Given Name	Meiju
	Suffix	
	Division	School of Computer Science
	Organization	Qinghai Normal University
	Address	Xining, 810008, Qinghai, China
	Email	1143828260@qq.com
Author	Family Name	Li
	Particle	
	Given Name	Keqin
	Suffix	
	Division	Department of Computer Science
	Organization	State University of New York
	Address	New Paltz, NY, 12561, USA
	Email	lik@newpaltz.edu
Abstract	Underwater Acoustic Networks (UANs) use acoustic communication and are characterized by limited bandwidth capacity, high energy consumption, long propagation delay, which cause the traditional protocols designed for radio channels to be either inapplicable or to be inefficient for UANs. The chapter introduces a three-layer protocol architecture for UANs which is Micro-ANP (including Application, Network-transport, and Physical layer). Further, based on the Micro-	

ANP architecture and Recursive LT (RLT) code, a handshake-free reliable transmission mechanism is presented in detail.

Chapter 10

Reliable Transmission Protocol for Underwater Acoustic Networks

Xiujuan Du, Meiju Li, and Keqin Li

10.1 Challenges of UANs

Recently, Underwater Acoustic Networks (UANs) research has attracted significant attention due to the potential for applying UANs in environmental monitoring, resource investigation, disaster prevention, and so on [1–10]. UANs use acoustic communication, but the acoustic channel is characterized by high bit errors (on the order of magnitude of 10^{-3} – 10^{-7}), long propagation delay (at a magnitude of a few seconds), and narrow bandwidth (only scores of kbps). The result is that the terrestrial-based communication protocols are either inapplicable or inefficient for UANs. Compared with conventional modems, the acoustic modems used in UANs consume more energy. However, the nodes are battery-powered and it is considerably more difficult to recharge or replace nodes in harsh underwater environments. Furthermore, underwater nodes are usually deployed sparsely, move passively with water currents or other underwater activity, and some nodes will fail due to energy depletion or hardware faults; therefore the network topology of UANs usually changes dynamically, which causes significant challenges in designing protocols for UANs.

X. Du (✉)

School of Computer Science, Qinghai Normal University, Xining, 810008, Qinghai, China

Key Laboratory of the Internet of Things of Qinghai Province, Guihan, China

e-mail: dxj@qhnu.edu.cn

M. Li

School of Computer Science, Qinghai Normal University, Xining, 810008, Qinghai, China

e-mail: 1143828260@qq.com

K. Li

Department of Computer Science, State University of New York, New Paltz, NY, 12561, USA

e-mail: lik@newpaltz.edu

© Springer International Publishing AG 2017

K. Daimi (ed.), *Computer and Network Security Essentials*,

DOI 10.1007/978-3-319-58424-9_10

Applications of UANs in areas such as business, scientific research, and military are usually sensitive: outsiders are not allowed to access the sensitive information, and anonymous secure communication is broadly applied. However, thus far, to the best of our knowledge, there are few papers concerning secure communications protocols for UANs [11–14]. The nature of opening and sharing of underwater acoustic channel makes communications inherently vulnerable to eavesdropping and interference. Because of the highly dynamic nature of UANs, as well as their lack of centralized management and control, designing secure routing protocols that support anonymity and location privacy is a large challenge.

In UANs with dynamic topology and impaired channel, network efficiency following the traditional five-layered architecture was obtained by cross-layer designs, which cause numerous complicated issues that are difficult to overcome. The chapter introduces a three-layer protocol architecture for UANs, which includes application layer, network-transport layer, and physical layer and is named Micro-ANP. Based on the three-layer Micro-ANP architecture, the chapter provides a handshake-free Media Access Control (MAC) protocol for UANs, and achieves reliable hop-by-hop transmissions.

The remainder of the chapter is organized as follows. Section 10.2 presents the Micro-ANP architecture. Section 10.3 reviews the research on reliable transmission mechanism so far. Section 10.4 details the handshake-free reliable transmission protocol for UANs based on Micro-ANP architecture and RLT code. Section 10.5 makes a conclusion and has a discussion about new trends of UANs research.

10.2 Micro-ANP Architecture

The majority of research on UANs has focused primarily on routing or MAC protocols, and few studies have investigated protocol architecture for UANs. The energy, computation, and storage resources of UANs are seriously constrained; consequently, the protocol stack running on UANs nodes should not be complicated. However, most research on UANs so far has followed the traditional five-layered architecture in network design, and in tough condition such as dynamic topology, seriously impaired channel, and scarce resources, network efficiency was obtained by cross-layer designs, which cause numerous complicated issues that are difficult to overcome. UANs need a simple and efficient protocol architecture. Du et al. provided a three-layered Micro-ANP architecture for UANs, which is composed of an application layer, a network-transport layer, and a physical layer as well as an integrated management platform, as shown in Fig. 10.1 [15].

The network-transport layer in Micro-ANP is primarily responsible for reliable hop-by-hop transmission, routing, and channel access control. In Micro-ANP, broadcasting, Level-Based Adaptive Geo-Routing (LB-AGR), and a secure anonymous routing are the three major routing protocols that are applicable to dynamic underwater topology [7, 16]. A secure anonymous routing protocol can achieve anonymous communication between intermediate nodes as well as two-way

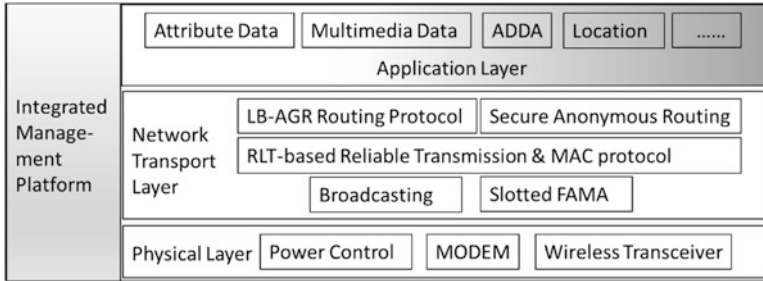


Fig. 10.1 Micro-ANP architecture

Table 10.1 Head fields of micro-ANP

Bits: 8	8	8	2	6	1	1	24	8	
Level of sender	Sender ID	Receiver ID	Type 00: Data 01: Ack 10: Control	Frame sequence number	Immediately ack 1: yes 0: no	If block 1: Yes 0: No	IDs of original packets	Block ID	13.1
Bits: 6	1	2	1	48	4	8	Variable	16	13.2
Block size	Direction 0: down 1: up	Sink ID	(Source destination) 0: position 1: node ID	(Source destination) position or ID Full "1" for broadcast	Application priority (application type)	Load length	Data	FCS	13.3

authentication between source and destination nodes without any real-time online Public Key Generator (PKG), thus decreases the network delay while improving network scalability. In Micro-ANP, slotted Floor Acquisition Multiple Access (slottedFAMA) and a RLT Code-based Handshake-Free (RCHF) reliable MAC protocol are the two-channel access control mechanism [9, 17].

Micro-ANP is a three-layered architecture that allows intermediate nodes to perform Application Dependent Data Aggregation (ADDA) at the application layer. Without requiring a cross-layer design, Micro-ANP can make efficient use of scarce resources. Moreover, Micro-ANP eliminates inapplicable layers and excessive repeated fields such as address, ID, length, Frame Check Sequence (FCS), and so on, thus reducing superfluous overhead and energy consumption. The head fields of the network-transport layer are listed in Table 10.1.

The application priority field is used to distinguish between different applications as shown in Table 10.2. This is because different applications have different priorities and require different Quality of Service (QoS) and their messages are transmitted using different routing decisions. Other fields in Table 10.2 will be explained in the respective protocol overview of the network-transport layer.

Table 10.2 Application priority

Priority	Upper protocol	Priority	Upper protocol
0	Attribute data	4	Video
1	Integrated management	5	Emergency alarm
2	Image	6	
3	Audio	7	

From Table 10.1, we can see that the common head-length of Micro-ANP is less than 20 bytes. In comparison, the total head-length of well-known five-layer models is more than 50 bytes. Therefore, Micro-ANP protocol greatly improves data transmission efficiency.

10.3 Overview of Reliable Transmission Mechanism

Considering the challenges for UANs, the existing solutions of terrestrial Radio Frequency (RF) networks cannot be applied directly to UANs, regardless of the MAC mechanism used, the reliability of data transmission, or the routing protocol. Sustained research work over the last decade has introduced new and efficient techniques for sensing and monitoring marine environments; several issues still remain unexplored. The inapplicability of conventional reliable transport mechanisms in UANs is analyzed as follows:

1. The high bit error rates of acoustic channels lead to high probability of packet erasure and a low probability of success in hop-by-hop transfers. Therefore, traditional end-to-end reliable transport mechanisms may incur too many re-transmissions and experience too many collisions, thus reducing channel utilization.
2. The low propagation speed of acoustic signals leads to long end-to-end delays, which causes issues when controlling transmissions between two end-nodes in a timely manner.
3. The Automatic Repeat Request (ARQ) mechanism re-transmits lost packets, but it requires an ACK (acknowledgement) for packets received successfully. It is well known that the channel utilization of the simple stop-and-wait ARQ protocol is very low in UANs due to long propagation delays and low bit rates. In addition, acoustic modems adopt half-duplex communication, which limits the choices for efficient pipelined ARQ protocols. Even worse, if the ACKs are lost, the successfully received packets will be re-transmitted by the sender, further increasing the bandwidth and energy consumed.

Some reliable transport protocols resort to Forward-Error-Correcting (FEC) to overcome the inherent problems with ACKs. FEC adopts erasure codes and redundancy bits. The payload bits of FEC are fixed prior to transmission. Before

transmitting, the sender encodes a set of n original packets into a set of N ($N \geq n$) 110
encoded packets. Let $m = N - n$, and m redundant packets are generated. To 111
reconstruct the n original packets, the receiver must receive a certain number (larger 112
than n) of encoded packets. The stretch factor is defined as N/n , which is a constant 113
that depends on the erasure probability. However, the error probability of UANs 114
channels is dynamic; overestimated error probability will incur additional overhead 115
and underestimated error probability will lead to transmission failure. 116

Reed and Solomon proposed the Reed–Solomon code based on some practical 117
erasure codes [18]. Reed–Solomon code is efficient for small n and m values. 118
However, the encoding and decoding algorithms require field operations, resulting 119
in a high computation overhead that is unsuitable for UANs due to the nodes' 120
limited computational capabilities. Luby et al. studied a practical Tornado code 121
which involves only XOR operations [19]. In addition, the encoding and decoding 122
algorithms are faster than those used for Reed–Solomon code. However, the 123
Tornado code uses a multi-layer bipartite graph to encode and decode packets, 124
resulting in a high computation and communication overhead for UANs. Xie et 125
al. presented a Segmented Data Reliable Transfer (SDRT) protocol [20]. SDRT 126
adopts Simple Variant of Tornado (SVT) code to improve the encoding/decoding 127
efficiency. Nevertheless, after pumping the packets within a window into the channel 128
quickly, the sender sends the packets outside the window at a very slow rate until it 129
receives a positive feedback from the receiver, which reduces channel utilization. 130
Mo et al. investigated a multi-hop coordinated protocol for UANs based on the 131
GF(256) random-linear-code to guarantee reliability and efficiency [21]. However, 132
the encoding vectors are generated randomly; consequently, the probability of 133
successfully recovering K data packets from K encoded packets could not be 134
guaranteed. Moreover, the decoding complexity was higher than other sparse codes. 135
Furthermore, the multi-hop coordination mechanism requires time synchronization 136
and is restricted to a string topology in which there is a single sender and a single 137
receiver. 138

Digital fountain codes are sparse codes on bipartite graphs that have high 139
performance [21, 23]. They are rate-less, i.e., the amount of redundancy is not 140
fixed prior to transmission and can be determined on the fly as the error recovery 141
algorithm evolves. These codes are known to be asymptotically near-optimal 142
for every erasure channel, and they allow for lightweight encoder and decoder 143
implementations. Luby proposed the LT code, in which the decoder is capable of 144
recovering the original symbols at a high probability from any set of output symbols 145
whose size is close to the originals [24]. However, the LT code was designed for 146
large numbers of data packets, which is not typically the case in UANs—especially 147
for mobile networks where the transmission time between two nodes is very limited 148
because of node mobility. Furthermore, the degree distribution used in LT code 149
results in a large number of nodes in the graph, causing a large overhead for each 150
packet. 151

10.4 Reliable Transmission Protocol for UANs

152

In this section, based on digital fountain code, a Recursive LT (RLT) code with a small degree distribution is proposed along with a reliable and handshake-free MAC protocol called as RCHF MAC protocol.

153
154
155

10.4.1 RLT Code

156

The coding scheme can greatly impact system performance. In this section, we present a Recursive LT (RLT) code, which achieves fast encoding and decoding. Given that packet loss is independent, we use a bipartite graph $G = (V, E)$ with two levels to represent the RLT code, where E is the set of edges and V is the set of nodes in the graph. $V = D \cup C$, where D is the set of input packets and C is the set of encoded packets. The edges connect the nodes in D and C .

157
158
159
160
161
162

1. Encoding

163

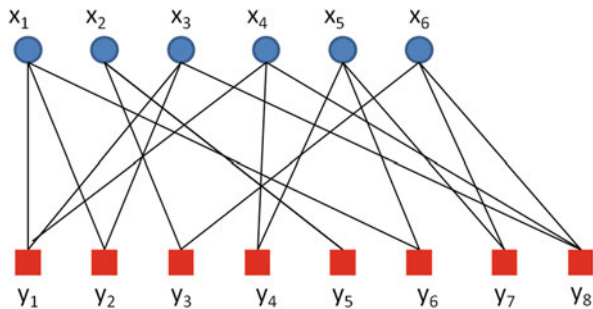
Consider a set of k input (original) packets, each having a length of l bits. The RLT encoder takes k input packets and can generate a potentially infinite sequence of encoded packets. Each encoded packet is computed independently of the others. More precisely, given k input packets $\{x_1, x_2, \dots, x_k\}$ and a suitable probability distribution $\Omega(d)$, a sequence of encoded packets $\{y_1, y_2, \dots, y_j, \dots, y_n\}, n \geq k$, are generated as shown in Fig. 10.2. The parameter d is the degree of the encoded packets—the number of input packets used to generate the encoded packets and $d \in \{1, 2, \dots, k\}$ (e.g., the degree of packet y_2 is 2 while the degree of packet y_8 is 3 in Fig. 10.2).

164
165
166
167
168
169
170
171
172

To restore all the k original packets at the receiver, the number of encoded packets received successfully is subject to be greater than k . Let $n = (k + \xi)/(1 - P_p)$; here, P_p is the erasure probability of an underwater acoustic channel (i.e., the PER), and $\xi (\xi > 0)$ corresponds to the expected number of redundant encoded packets received. The ξ redundant packets are used to decrease the probability that the

173
174
175
176
177

Fig. 10.2 Encoding graph of RLT code




AQ3

receiver fails to restore the original k input packets in only one transmission phase. 178
 The sequence of encoded packets is $y_1, y_2, \dots, y_j, \dots, y_n \in C$. The RLT encoding 179
 procedure is as follows: 180

- a. From D , the set of input packets, successively XOR the k packets to generate one encoded packet with degree k , then duplicate the packet to obtain $\lceil 1/(1 - P_p) \rceil$ copies. 181-183
- b. From set D , select $\lceil m/(1 - P_p) \rceil$ distinct packets randomly to constitute a seed set S_1 , and generate $\lceil m/(1 - P_p) \rceil$ encoded packets with degree one. Here, m is the expected number of encoded packets received successfully with degree one. In reality, we can set $1 \leq m \leq \max(\lfloor k/4 \rfloor, 1)$. 184-187
- c. Let $S_2 = D - S_1$. From the set S_2 , uniformly select $\lceil k/(2(1 - P_p)) \rceil$ input packets at random, and perform the XOR operation, randomly selecting one packet in the set S_1 to generate $\lceil k/(2(1 - P_p)) \rceil$ encoded packets with degree two. 188-190
- d. Let $S_3 = D - S_1 - S_2$. If S_3 is not null, select $\lceil k/(6(1 - P_p)) \rceil$ input packets at random from set S_3 ; otherwise, from set D , perform the XOR operation using one packet from S_2 and another from S_1 to generate $\lceil k/(6(1 - P_p)) \rceil$ encoded packets with degree three. 191-194
- e. Let $S_4 = D - S_1 - S_2 - S_3$. If S_4 is not null, randomly select $\lceil (\xi + k/3 - m - 1)/(1 - P_p) \rceil$ input packets from set S_4 ; otherwise, from set D , perform the XOR operation using three packets from S_1, S_2 , and S_3 , respectively, to generate $\lceil (\xi + k/3 - m - 1)/(1 - P_p) \rceil$ encoded packets with degree four. 195-198

2. Decoding 199

When an encoded packet is transmitted over an erasure channel, it is either received successfully or lost. The RLT decoder tries to recover the original input packets from the set of encoded packets received successfully. The decoding process of RLT is as follows: 200-203

- a. Find an encoded packet y_j which is connected to only one input packet x_i . If the receiving node fails to find any such encoded packet, stop decoding. 204-205
- b. Set $x_i = y_j$. 206
- c. Set $y_m = y_m \oplus x_i$ for each encoded packet which is connected to x_i , denoted by y_m . Here, \oplus indicates the XOR operation. 207-208
- d. Remove all the edges connected to x_i . 209
- e. Go to Step 1.  210

3. Degree distribution. 211

The limited delivery time between two nodes caused by node mobility leads to the constraint that digital fountain codes must work with small k values in UANs communications. In RLT, to reconstruct the input packets, the degree distribution of the received encoded packets should have the following properties: 212-215

- a. The received encoded packets should connect all the input packets. 216
- b. The process of encoding and decoding should not involve too many XOR operations. 217-218
- c. At least one encoded packet with degree one should be successfully received by the receiver. 219-220

Given the high bit error, P_b , which is on the order of magnitude of 10^{-3} – 10^{-7} , the PER, P_p , is given by Eq. (10.1):

$$p_p = 1 - (1 - p_b)^l, \quad (10.1)$$

where l is the packet size. As discussed earlier, in Micro-ANP architecture, the optimal packet size is greater than 100 bytes, and P_p is non-negligible in Eq. (10.1). Considering the k input packets, to address the properties of degree distribution discussed above, the degree distribution of the encoded packets in the sending nodes is given by Eq. (10.2):

$$\Omega(d) = \begin{cases} \frac{m}{\xi+k}, & d = 1; \\ \frac{k}{d(d-1)(\xi+k)}, & d = 2, 3; \\ \frac{\xi+(1/3)k-(m+1)}{\xi+k}, & d = 4; \\ \frac{1}{\xi+k}, & d = k; \end{cases} \quad (10.2)$$

where $\sum_d \Omega(d) = 1$.

Lemma 1 The average degree of encoded packets $\lambda \approx 3.7$.

Proof From the degree distribution given by Eq. (10.2), we obtain:

$$\begin{aligned} \lambda &= E(d) = \sum_{d=1}^4 (d \times \Omega(d)) \\ &= \frac{1 \times m}{\xi+k} + \frac{2 \times k}{2 \times 1 \times (\xi+k)} + \frac{3 \times k}{3 \times 2 \times (\xi+k)} \\ &\quad + \frac{4 \times (\xi + 1/3k - (m+1))}{\xi+k} + \frac{k}{\xi+k} \\ &= 3\frac{2}{3} + \frac{3m-4}{\xi+k}. \end{aligned}$$

Usually, $|(\xi/3) - 3m - 4| \ll |\xi + k|$, so $\lambda \approx 3\frac{2}{3} \approx 3.7$.

Given the block size k , from Lemma 1, we can derive the decoding complexity of RLT is about $3.7k$, which is linear to the number of input packets. A comparison of the encoding/decoding complexity of various codes is shown in Table 10.3.

In this section, based on the digital fountain code, we propose a Recursive LT (RLT) code with small degree distribution, and introduce the erasure probability of channel P_p into the RLT code for the first time to improve the decoding probability at the receiving node. RLT is applicable to dynamic UANs with limited transmission time between two nodes; it reduces the overhead of encoding and decoding and substantially improves the efficiency of decoding process.

Table 10.3 Decoding complexity comparison

Code	Encoding/decoding complexity	
GF (256) in [21]	$O(k^3)$	18.1
LT	$k \ln_e^k$	18.2
SDRT in [20]	$k \cdot \ln(1/\epsilon)$	18.3
RS	$k(N-k) \log_2^N$	18.4
RLT	$3.7k$	18.5

10.4.2 RCHF: RLT Code-Based Handshake-Free Reliable Transmission Protocol 242
243

After solving the problems of degree distribution, encoding and decoding of RLT in advance, a reliable RLT-based media access control protocol should be presented that nodes can use to communicate in real time. Wireless transceivers usually work in half-duplex mode: a sending node equipped with a single channel is unable to receive packets while it is transmitting; therefore, the RCHF solution is supposed to avoid interference caused by transmitting to a node in a sending state. So far, in MAC solutions of wireless multi-hop packet networks, an RTS/CTS handshake is used to dynamically determine whether the intended receiver is ready to receive a frame. For underwater sensors, the rate at which data bits can be generated is approximately 1–5 bps and the optimal packet-load for UANs is about 100 bytes. In contrast, the length of an RTS frame is a few dozen bytes. Therefore, RTS/CTS frames are not particularly small compared with data frames; consequently, the benefits from using RTS/CTS handshake are unremarkable. Moreover, considering the characteristics of acoustic communication (i.e., low bandwidth, long propagation delay, etc.), RTS/CTS handshake decreases channel utilization and network throughput dramatically while prolonging end-to-end delay. Therefore, coupled closely with the RLT code, we propose a RCHF protocol which is a state-based handshake-free reliable MAC solution for UANs. 244
245
246
247
248
249
250
251
252
253
254
255
256
257
258
259
260
261

10.4.2.1 Reliable Transmission Mechanism 262

In the RCHF MAC solution, a source node first groups input packets into blocks of size k (i.e., there are k input packets in a block). Then, the source node encodes the k packets, and sends the encoded packets to the next hop. When k is equal to 50, the minimum time interval for transmitting a block between two neighbor nodes is approximately 60 s, which is in compliance with the requirements of the limited transmission time between two neighbor nodes in dynamic UANs. By setting the block size k appropriately, RCHF can control the transmission time, allowing the receiver to be able to receive sufficient encoded packets to reconstruct the original block even when the nodes are moving. Application data are transferred from a source node to a sink node block by block and each block is forwarded via RLT coding hop-by-hop. 263
264
265
266
267
268
269
270
271
272
273

In the RCHF protocol, a node sending packets is considered to be in the transmission phase. To facilitate receiving an ACK for transmitted packets, avoid conflicts between transmitting and receiving, and compromise between transmission efficiency and fairness, two transmission constraints are defined as follows:

1. The maximum number of data frames allowed to be transmitted in one transmission phase is N_{\max} .
2. The minimum time interval between two tandem transmission phases of the same node is T_a . The node waiting for T_a expiration is considered to be in a send-avoidance phase. At present, underwater acoustic modems are half-duplex, the delay for state transition between sending and receiving usually ranges from hundreds of milliseconds to several seconds, which is close to the magnitude of the maximum round-trip time (RTT) [18]. Therefore, to facilitate the receiver to switch to the sending state to transmit the ACK, we set $T_a = 2 \times RTT$.

After transmitting N ($N \leq N_{\max}$) encoded packets, the sender switches to the receiving state and waits for the receiver's ACK. To have a high probability of being able to reconstruct the original k input packets at the receiver, the number of encoded packets received successfully is supposed to be larger than k , denoted as $k + \xi$. Considering the high packet error rate, P_p , we set $N = (k + \xi)/(1 - P_p)$. The parameter ξ , ($\xi > 0$) is fixed and corresponds to the expected number of redundant encoded packets the receiver will receive. The ξ redundant packets are used to decrease the probability that the receiver fails to restore the original k input packets in the transmission phase, and the factor $1/(1 - P_p)$ is used to compensate for channel errors.

The ACK frame includes the number of frames received at the receiver as well as the indices of unrecovered input packets. The number of frames received successfully can be used to update the packet error rate P_p on the fly. If the receiver can reconstruct the whole block, it sends back an ACK with "null" in the index field.

Given k_1 input packets unrecovered after the previous transmission phase, the sender encodes and transmits N_1 encoded packets with the degree distribution given by Eq. (10.2) in which k is replaced by k_1 . $N_1 = (k_1 + \xi)/(1 - P_p)$. Then the sender collects the feedback from the receiver again. This process repeats until the sender receives an ACK with "null" in the index field.

10.4.2.2 State-Based Handshake-Free Media Access Control

After network initialization, each node maintains one dynamic neighbor table that includes a state field containing the real-time state of neighbor nodes as shown in Table 10.4. Here, state "0" indicates that the neighbor node is in sending state, state "1" indicates that the neighbor node is receiving frames from other nodes, "2" denotes an unknown state, and "3" means the neighbor node is in the send-avoidance phase.

The format of frames in our protocol is shown in Table 10.5. The level field contains the forwarder's level, the frame sequence number is used to identify the

Table 10.4 The state table of neighbor nodes

Value	State	
0	Sending state	t10.1
1	Receiving frame from other nodes	t10.2
2	Unknown state	t10.3
3	Transmission-avoidance	t10.4

Table 10.5 The format of data frame

Bits: 8	8	8	2	6	1	1	
Level of sender	Sender ID	Receiver ID	Type 00: Data 01: Ack 10: Control	Frame sequence number	Immediately ack 1: yes 0: no	If block 1: Yes 0: No	t13.1
Bits:24	8	6	–	8		Variable	t13.2
IDs of original packets	Block ID	Block size	–	Load length		Data	t13.3

frame in one frame-sequence during one transmission phase, the original packet ID field is used to indicate the IDs of packets that are XORed, and the immediate ACK field is used to inform the receiver whether to return an ACK immediately, where “1” means “yes” and “0” means “no.” The first nine bytes are used by the RCHF MAC protocol to realize reliable transmission hop-by-hop; the fields are updated hop-by-hop. The fields from the tenth to the sixteenth bytes are used by the LB-AGR routing protocol and are omitted here for simplicity.

When a node has packets to send, it searches the neighbor table for the state field of the intended receiver. If the state is “0” or “1,” it will delay delivery until the state is greater than one; otherwise, the node becomes a sender, switches into the transmission phase, and starts to deliver frames. The pseudocode for sending packets is omitted.

10.4.3 Simulation Result of RCHF

In this section, we evaluate the performance of the RCHF protocol by simulation experiments. All simulations are performed using Network Simulator 2 (NS2) with an underwater sensor network simulation package extension (Aqua-Sim). Our simulation scenario is similar to reality; 100 nodes are distributed randomly in an area of 7000 m × 7000 m × 2000 m. The simulation parameters are listed in Table 10.6.

The protocol is evaluated in terms of average end-to-end delay, end-to-end delivery ratio, energy consumption, and throughput. We define the delivery ratio and throughput of the RCHF protocol as follows:

Table 10.6 Simulation parameters

Parameter	Value	
Block size k	50	t15.1
Packet length l	160 bytes	t15.2
Bandwidth	10 kbps	t15.3
Routing protocol	Static	t15.4
Traffic	CBR	t15.5
Transmission range	1500 m	t15.6
MAC protocol	802.11	t15.7

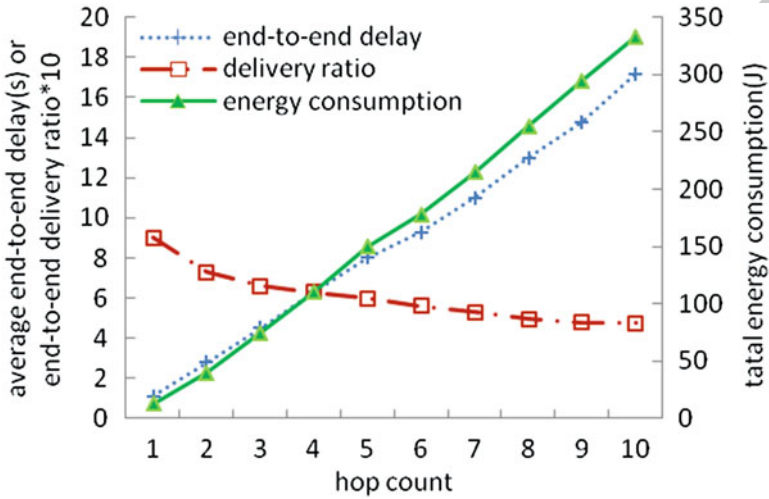


Fig. 10.3 Performance vs. hop COUNT

1. The end-to-end delivery ratio is defined by Eq. (10.3):

337

$$\text{end-to-end delivery ratio} = \frac{\text{\#of packets received successfully at sink}}{\text{\#of packets generated at sources}} \quad (10.3)$$

338

2. The throughput is defined as the number of bits delivered to the sink node per second (bps)

339

340

As shown in Fig. 10.3, the end-to-end delivery ratio of the RCHF protocol is close to “1” when the hop count is “1” and decreases slightly as the hop count increases, which is considered good performance for UANs from a delivery ratio aspect. Figure 10.3 also shows that the end-to-end delay and total energy consumption rise with the hop count which is understandable. Note that the real value of the end-to-end delivery ratio is the value of the ordinate axis divided by 10.

341

342

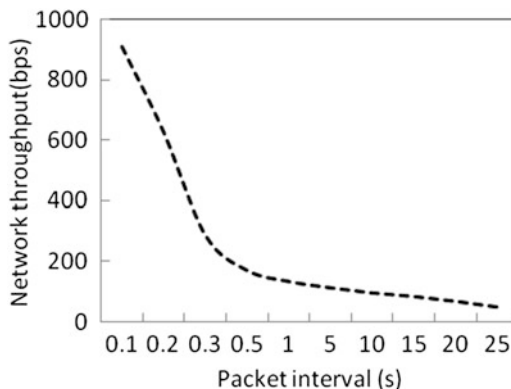
343

344

345

346

Fig. 10.4 Throughput vs. packet interval(s)



As shown in Fig. 10.4, the network throughput of RCHF decreases as the interval 347
 time between two successive packets generated by the source node increases. This 348
 occurs because as the interval time increases, fewer packets are generated, which 349
 reduces the network load. 350

10.5 Conclusion 351

In this chapter, a three-layer Micro-ANP protocol architecture for UANs is intro- 352
 duced. Further, a kind of digital fountain code which is called as RLT is presented. 353
 RLT is characterized by small degree distribution and recursive encoding, so RLT 354
 reduces the complexity of encoding and decoding. Based on the Micro-ANP 355
 architecture and RLT code, a handshake-free reliable transmission mechanism- 356
 RCHF is presented. In RCHF protocol, frames are forwarded according to the state 357
 of the receiver which can avoid the sending-receiving collisions and overhearing 358
 collisions. Simulations show that RCHF protocol can provide higher delivery ratio, 359
 throughput, and lower end-to-end delay. 360

As a new trend, how to combine the specific underwater application scenarios, 361
 transform the negative factors of UANs into favorable factors is an interesting 362
 research. For example, the mobility of nodes brings about extra routing overhead, 363
 and reduces end-to-end performance. However, the mobility of Autonomous Under- 364
 water Vehicle (AUV) and the policy of cache-carry-forward help to improve the data 365
 forwarding rate. 366

Meanwhile, under the precondition of less resource consumption, guaranteed 367
 channel utilization and network throughput, combining the technologies of channel 368
 coding, cognitive underwater acoustic communication, data compression, and post- 369
 quantum public key cryptography, studying on secure and reliable data transmission 370
 is another future work. 371

Acknowledgments This work is supported by the National Natural Science Foundation Projects 372 of China (61162003), Key Laboratory of IoT of Qinghai Province, Qinghai Office of Science 373 and Technology (2015-ZJ-904), Hebei Engineering Technology Research Center for IOT Data 374 acquisition & Processing. 375

References

376

1. Zhou, Z., Peng, Z., Cui, J. H., & Jiang, Z. (2010). Handling triple hidden terminal problems for 377 multi-channel MAC in long-delay underwater sensor networks. In *Proceedings of international 378 conference on computer communications (INFOCOM)* (pp. 1–21). San Diego, USA: IEEE 379 Computer Society. 380
2. Pompili, D., & Akyildiz, I. F. (2010). A multimedia cross-layer protocol for underwater 381 acoustic sensor networks. *IEEE Transaction on Wireless Communications*, 9(9), 2924–2933. 382
3. Pompili, D., Melodia, T., & Akyildiz, I. F. (2010). Distributed routing algorithms for 383 underwater acoustic sensor networks. *IEEE Transaction on Wireless Communications*, 9(9), 384 2934–2944. 385
4. Huang, C. J., Wang, Y. W., & Liao, H. H. (2011). A power-efficient routing protocol for 386 underwater wireless sensor networks. *Applied Soft Computing*, 11(2), 2348–2355. 387
5. Zhou, Z., & Cui, J. H. (2008). Energy efficient multi-path communication for time-critical 388 applications in underwater sensor networks. In *Proceedings of the 9th ACM international 389 symposium on mobile ad hoc networking and computing*, Hong Kong, China (pp. 1–31). New 390 York, USA: ACM. 391
6. Hao, K., Jin, Z., Shen, H., & Wang, Y. (2015). An efficient and reliable geographic routing 392 protocol based on partial network coding for underwater sensor networks. *Sensors*, 15, 12720– 393 12735. 394
7. Du, X., Huang, K., & Lan, S. (2014). LB-AGR: Level-based adaptive geo-routing for under- 395 water sensor networks. *The Journal of China Universities of Posts and Telecommunications*, 21(1), 54–59. 396 397
8. Du, X., Peng, C., Liu, X., & Liu, Y. (2015). Hierarchical code assignment algorithm and state- 398 based CDMA protocol for UWSN. *China Communications*, 12(3), 50–61. 399
9. Du, X., Li, K., Liu, X., Su, Y. (2016) RLT code based handshake-free reliable MAC protocol for 400 under-water sensor networks. *Journal of Sensors*. doi:10.1155/2016/3184642 401
10. Du, X., Liu, X., & Su, Y. (2016). Underwater acoustic networks testbed for ecological 402 monitoring of Qinghai Lake. In *Proceedings of oceans16 Shanghai* (pp. 1–10). 403
11. Dong, Y., & Liu, P. (2010). Security consideration of underwater acoustic networks. In 404 *Proceedings of International Congress on Acoustics, ICA*. 405
12. Cong, Y., Yang, G., Wei, Z., & Zhou, W. (2010). Security in underwater sensor network. In 406 *Proceedings of international conference on communication and mobile computing* (pp. 162– 407 168). 408
13. Dini, G., & Lo Duca, A. (2011). A cryptographic suite for underwater cooperative applications. 409 In *Proceedings of IEEE symposium on computers & communications* (pp. 870–875). 410
14. Peng C., Du X., Li K., & Li M.. (2016) An ultra lightweight encryption scheme in underwater 411 acoustic networks. *Journal of Sensors*. doi:10.1155/2016/8763528 412
15. Du, X. 2014 Micro-ANP protocol architecture for UWSN. China Patent ZL201210053141.0. 413
16. Molins, M., & Stojanovic, M. (2006). Slotted FAMA: A MAC protocol for underwater acoustic 414 networks. In *Proceedings of IEEE OCEANS'06* (pp. 16–22), Singapore. 415
17. Reed, I., & Solomon, G. (1960). Polynomial Codes over certain finite fields. *Journal of the 416 Society for Industrial and Applied Mathematics*, 8(2), 300–304. 417
18. Luby, M., Mitzenmacher, M., Shokrollahi, A., & Spielman, D. (1997). Practical loss-resilient 418 codes. In *ACM STOC* (pp. 150–159). 419

19. Xie, P., Zhou, Z., Peng, Z., Cui, J., & Shi, Z. (2010). SDRT: A reliable data transport protocol for underwater sensor networks. *Ad Hoc Networks*, 8(7), 708–722. 420–421
20. Mo, H., Peng, Z., Zhou, Z., Zuba, M., Jiang, Z., & Cui, J. (2013). Coding based multi-hop coordinated reliable data transfer for underwater acoustic networks: Design, implementation and tests. In *Proceedings of Globecom 2013, wireless network symposium* (pp. 5066–5071). 422–424
21. MacKay, D. J. C. (2005). Fountain codes. In *Proceedings of IEEE communications* (pp. 1062–1068). 425–426
22. Shokrollahi, A. (2006). Raptor codes. *Information theory. IEEE Transactions*, 52(6), 2551–2567. 427–428
23. Luby, M. (2002). LT codes. In *Proceedings of the 43rd annual IEEE symposium on foundations of computer science* (pp. 271–280). 429–430
24. Xie, P., Cui, J.-H., & Lao, L. (2006). VBF: Vector-based forwarding protocol for underwater sensor networks. In *Proceedings of IFIP networking*. 431–432
25. Yan, H., Shi, Z. J., & Cui, J. H. (2008). DBR: Depth-based routing for underwater sensor networks. In *Proceedings of IFIP networking* (pp. 72–86), Singapore. 433–434
26. Niculescu, D., & Nath, B. (2003). DV based positioning in ad hoc networks. *Journal of Telecommunication Systems*, 22(1/4), 267–280. 435–436

AQ5

UNCORRECTED PROOF

AUTHOR QUERIES

- AQ1. Please check the affiliation “3” and correct if necessary.
- AQ2. Please note that the Figures, Tables and Equations are present according to the section wise manner. To follow Springer style, We have to change as Chapter wise manner. Hence the changes are as follows, Fig. 2.1→Fig. 10.1, Fig. 4.1→Fig. 10.2, Fig. 4.2→Fig. 10.3, Fig. 4.3→Fig. 10.4, Table 2.1→Table 10.1, Table 2.2→Table 10.2, Table 4.1→Table 10.3, Table 4.2→Table 10.4, Table 4.3→Table 10.5, Table 4.4→Table 10.6, Eq. 4.1→Eq. 10.1, Eq. 4.2→Eq. 10.2, Eq. 4.3→Eq. 10.3
- AQ3. Please check the presentation of the list below, and correct if necessary.
- AQ4. Please check whether the edits made in Refs. [12, 22, 23] are correct.
- AQ5. Refs. [22, 25, 26] are not cited in the text. Please provide the citation or delete them from the list.